

# Femtosecond laser ablation ICP-MS†

Richard E. Russo, Xianglei Mao, Jhanis J. Gonzalez and Samuel S. Mao

Lawrence Berkeley National Laboratory, M/S 70-108B, Berkeley, CA 94720.

E-mail: Rerusso@lbl.gov; Fax: (510)486-7303; Tel: (510)486-4258

Received 27th February 2002, Accepted 27th May 2002

First published as an Advance Article on the web 14th June 2002

Femtosecond laser ablation was investigated for direct solid sample chemical analysis. The phonon relaxation time in a solid is of the order of 100 fs, which is the same as the laser pulse duration. For such excitation, there should be little time for the matrix to experience a “temperature” during the laser pulse. If the surface explodes before the photon energy is dissipated as heat in the lattice, the ablation process should produce stoichiometric vapor (elemental fractionation should be negligible). Based on this hypothesis, NIST glasses were ablated using 100 fs laser pulses at 800 nm, with subsequent elemental analysis using the ICP-MS. Pb and U intensities, and Pb/U ratios in the ICP, were measured during repetitively femtosecond-pulsed ablation. These data show that fluence (laser energy/spot area) has a significant influence on the amount of mass ablated and on the degree of fractionation. An optimal fluence was found at which the fractionation index approached unity; negligible fractionation. Infrared femtosecond laser ablation produced similar characteristics to UV nanosecond laser ablation.

## Introduction

The goal of laser ablation (LA) chemical analysis is to convert a small quantity of mass from a solid sample into vapor-phase constituents with an exact composition to the solid phase, and transport that vapor efficiently to an analytical source. For chemical analysis using laser ablation sampling, a primary concern has been non-stoichiometric generation of vapor, a process called fractionation.<sup>1–6</sup> There is significant evidence that fractionation is related to the laser properties, including the pulse duration, energy, and beam diameter. These laser-beam properties govern the processes underlying the release of vapor/particulates from the solid sample. Almost all previous analytical laser ablation work has utilized nanosecond pulsed lasers. Commercial laser ablation systems employing excimer or Nd:YAG laser have pulse durations approximately 30 ns or 6 ns, respectively.<sup>1–6</sup> For nanosecond laser-pulse ablation, there is ample time for photon energy to dissipate in the lattice as heat during the laser pulse. On the other hand, femtosecond lasers are finding widespread use in many applications because of their ability to ablate well-defined craters with minimal thermal heating to the surrounding area of the crater; most of the laser energy is converted into kinetic energy of the ablated vapor. For this reason, femtosecond lasers have been suggested as alternatives for laser ablation chemical analysis because of the potential for reduced fractionation.<sup>7–9</sup> The femtosecond laser-material interaction involves nonlinear processes, resulting from the very high intensity (on the order of  $10^{14}$  W cm<sup>-2</sup>) and the short time duration with respect to the phonon relaxation time in a solid material. At this high laser intensity, multiphoton and tunneling ionization processes may dominate the ablation interaction converting photon energy into kinetic energy and thereby minimizing heating of the lattice.<sup>10</sup> Heating of the sample prior to the explosive release of vapor may be one of the main causes of fractionation. Also, the femtosecond laser pulse will not interact with a plasma (vapor) of sample mass leaving the sample surface. The mass moves too slowly to escape the surface during the laser pulse, in contrast to the case for longer pulse (e.g. nanosecond) laser ablation in which

plasma shielding has been considered a mechanism of energy loss and a possible contributor to fractionation. The entire laser energy in the femtosecond pulse should be deposited into the sample surface region. Even though the femtosecond laser pulse energy is deposited in the sample and plasma shielding cannot exist, the high velocity ablated mass will establish a shock wave and plasma that occur after the laser pulse is finished. The recoil pressure from the shock wave and radiation heat transport from this plasma do contribute to heating of the sample and further mass ejection. The basis of this manuscript is to investigate how femtosecond laser ablation with these attributes would influence time dependent mass removal during repetitive laser pulsing and elemental fractionation.

Preliminary research using femtosecond lasers for analytical spectroscopy has only recently been reported,<sup>11–15</sup> partly due to the unavailability of reliable high power femtosecond lasers. These previous studies primarily addressed chemical analysis in the laser-induced breakdown (LIBS) plasma. In this paper, we investigated femtosecond laser ablation with sample transport to an inductively-coupled plasma mass spectrometer (ICP-MS). The effect of laser fluence on fractionation and calibration of Pb/U ratios is reported. NIST glasses were ablated using 100 fs laser pulses with 800 nm wavelength. Pb and U intensities, and Pb/U ratios were measured during repetitively pulsed femtosecond ablation.

## Experimental

The experimental system includes a femtosecond laser system (Spectra-Physics), a PQ3 ICP-MS (VG Elemental), and a laser ablation chamber (built in house). The femtosecond laser system includes a MaiTai femtosecond Ti:Sapphire seed laser, a Quanta-Ray and an Evolution nanosecond pump laser, and a TSA regenerative amplifier. The properties of this laser system are 25 mJ per pulse energy and 100 fs pulse duration at 10 Hz repetition rate. The laser-beam has a Gaussian energy profile across its diameter. A single plano-convex lens with a focal length of 20 cm was used to focus the laser beam onto the sample inside the ablation chamber. The ablation chamber was described in previous references.<sup>1,6</sup>

NIST 610 glass was used as the sample for the fluence studies. NIST 610, 612, 614, and 616 glasses were used for

†Presented at the 2002 Winter Conference on Plasma Spectrochemistry, Scottsdale, AZ, USA, January 6–12, 2002.

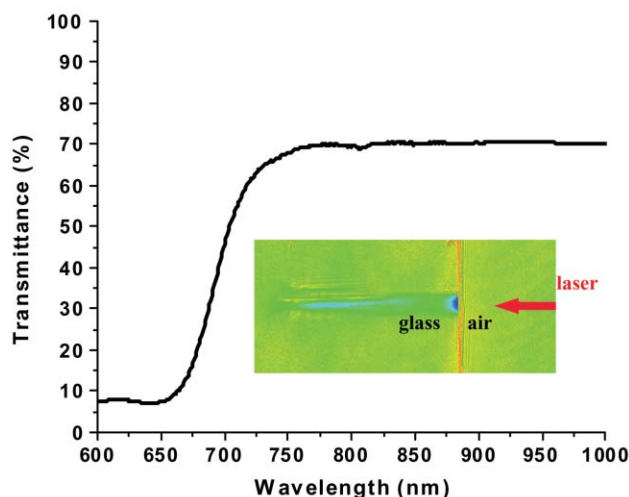


**Fig. 1** Transmittance of NIST 610 glass measured using a spectrophotometer. (a) The inset shows 800 nm transmission through the glass during excitation by a 100 fs pulse. (b) The dark filaments represent nonlinear changes in the absorption properties.

obtaining a calibration curve of the measured *versus* certified Pb/U ratios. The elemental concentrations in the NIST glasses can be found in refs. 16–18. ICP-MS signal intensity data were acquired in the time-resolved mode during repetitive ablation at a single sample surface location (crater formation). Background correction was applied to all measurements before calculating the ICP-MS intensities and elemental ratios. Crater diameters were measured using a white-light interferometric microscope (New View 200, Zygo Corporation).

## Results and discussion

The fundamental wavelength (800 nm) of the Ti:Sapphire laser was used for these studies. On the femtosecond time scale, linear optical absorption and transmission should not be primary parameters affecting ablation. At 800 nm laser wavelength, NIST 610 glass exhibits about 70% transmission (Fig. 1(a)) when measured using a spectrophotometer. However, this transmission value does not account for the nonlinear

interactions of the glass with a femtosecond laser pulse. A transmission image of 100 fs, 800 nm light propagation in a glass microscope slide provides evidence of the existence of nonlinear changes in optical properties (Fig. 1(b)). Femtosecond irradiation below the damage threshold incubates defects (electron-hole centers) in the lattice structure irreversibly changing the refractive index and optical properties. The filament-like structure results from nonlinear self-focusing during the femtosecond laser pulse. Even though the laser energy density (fluence) was below the damage threshold for ablation in this glass sample, the changes in optical properties are evident. Therefore, wavelength is not a well-defined parameter using femtosecond ablation, and direct comparisons should not be made to one-photon absorption. The data shown in Fig. 1 demonstrate how a sample that is nominally ‘transparent’ at 800 nm, can be absorbing using femtosecond excitation.

The 800 nm, 100 fs pulses were used to ablate the NIST glasses. In this work, ICP-MS intensities *versus* time represent repetitive ablation at a single sample location; as a crater is formed in the sample. Fig. 2 shows the ICP-MS time response for repetitively pulsed ablation of NIST 610 as a function of laser fluence. The fluence was changed by varying the laser-beam spot size on the sample surface, with fixed laser energy of approximately 0.8 mJ per pulse. Although only Pb and U intensities, and the Pb/U ratio are plotted, similar behavior was measured for other trace and matrix elements in the NIST samples. The change in ICP-MS intensity represents a change in the mass ablation rate (mass ablated per pulse). The ablation rate significantly depends on the laser fluence.

At low fluence ( $1.5 \text{ J cm}^{-2}$ ), the signal intensity initially increased and then decayed rapidly as the crater was formed. As the laser fluence was increased, the temporal response changed to a more gradual increase and decrease in the ablation rate. Similar time-dependent behaviors were measured previously using nanosecond UV pulsed ablation of transparent samples.<sup>1,6,7,19,20</sup> For nanosecond and femtosecond pulses, the ablation rate is strongly correlated to the fluence and crater properties. With UV nanosecond laser ablation, the initial high ablation rate (similar to Fig. 2 for the femtosecond pulses at  $1.5 \text{ J cm}^{-2}$ ) was related to the optical penetration depth, or the absorbed laser energy per unit volume.<sup>20</sup> The initial peak was

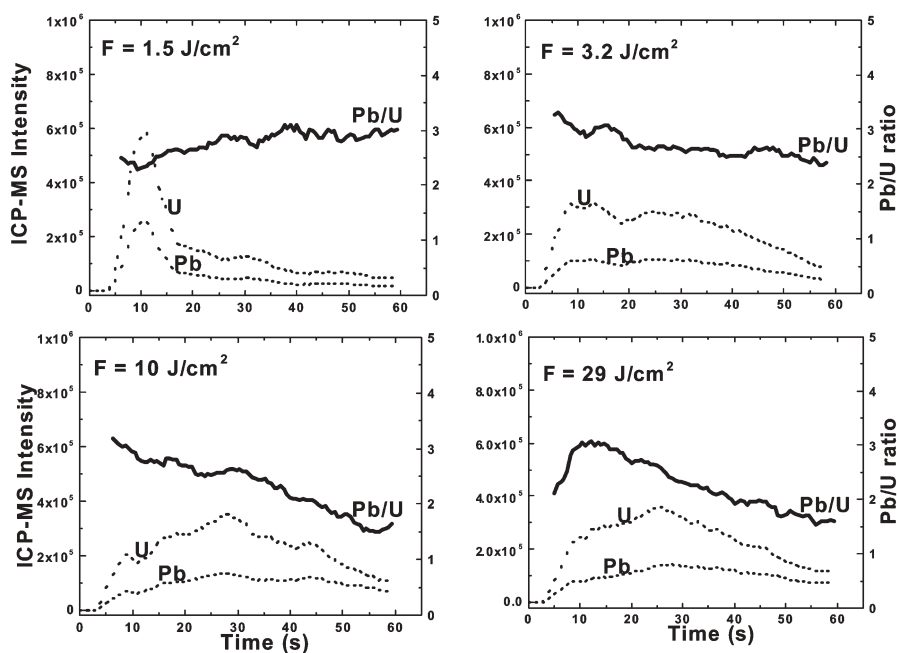


**Fig. 2** ICP-MS time-dependent Pb and U intensities, and Pb/U ratios *versus* laser fluence. 100 fs pulses at 10 Hz repetition rate. Single spot, crater formation.

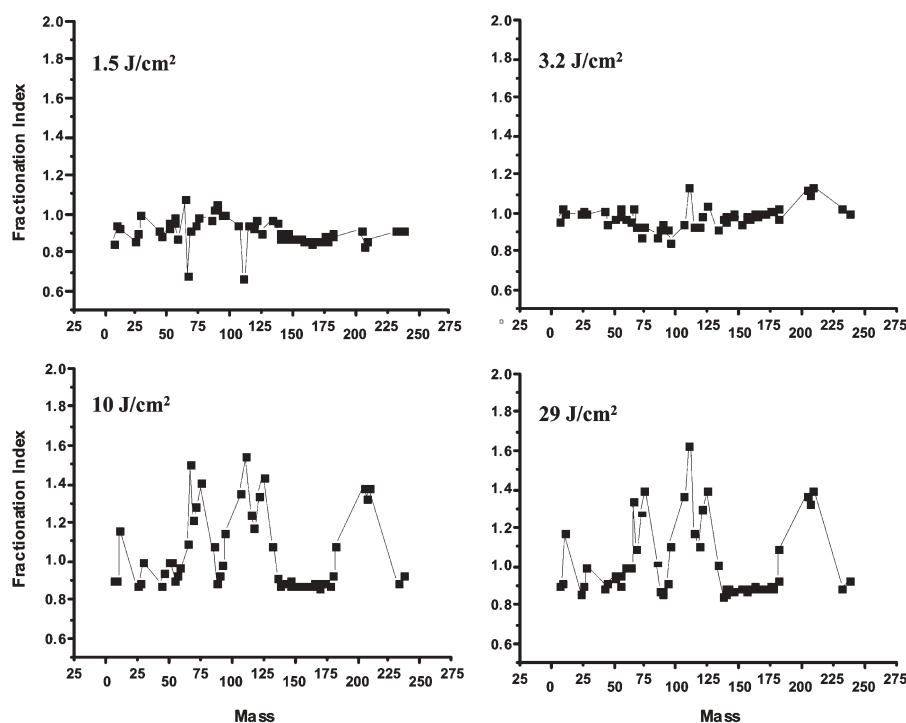


Fig. 3 Fractionation indices at four laser fluences for 800 nm 100 fs laser ablation of NIST 610 glass.

measured in transparent, but not opaque, NIST glasses. Also, increasing the laser fluence could minimize the initial peak, similar to that measured in this work using femtosecond pulses. A nonlinear absorption layer, rather than the linear optical penetration depth, may be responsible for the absence of the initial peak at higher fluences for femtosecond pulses. At high laser fluences, strong nonlinear absorption (*cf.* Fig. 1) exists for 100 fs ablation that could limit the laser energy deposition to within a layer immediately beneath the sample surface. The extent of such an absorption layer was found to be of the order of about  $1\ \mu\text{m}$ .<sup>7</sup> A general trend is that shorter laser pulse durations will induce a stronger nonlinear effect. The initial intensity peak would be suppressed at a lower fluence for shorter laser pulse durations, consistent with the literature in that a higher fluence ( $>20\ \text{J cm}^{-2}$ ) was required to minimize the initial peak using nanosecond laser ablation.

The change in the Pb/U temporal profile is related to fractionation, as a crater is formed in the sample.<sup>21,22</sup> As evident in Fig. 2, the behavior of the Pb/U ratio with time is a function of laser fluence. The absolute value of the ratio is dependent on several factors, including the laser fluence, ablated particle size distribution, transport efficiency, and ICP-MS response. Similar behavior was measured for nanosecond laser ablation.<sup>1,6</sup> The time-dependent Pb/U response is strongly related to crater formation, at each fluence. To characterize elemental fractionation for this case (repetitively pulsed ablation at a single sample location with the subsequent formation of a crater), the term fractionation index (FI) was defined. FI is plotted as a measured elemental ratio, normalized to a matrix element, in the last half of the ablation time divided by the normalized ratio in the first half of the ablation time.<sup>2</sup> In most cases, the first several seconds (called pre-ablation) of data are discarded. The value of the fractionation index generally depends on laser fluence, wavelength, pulse duration, and the sample properties. A value of unity would indicate no relative fractionation as the crater is formed.

Fractionation indices (normalized to Ca matrix element) were measured for most of the elements in NIST 610 glass. Fig. 3 shows that the fractionation index is strongly dependent on laser fluence. The fractionation indices at 10 and  $29\ \text{J cm}^{-2}$  are very similar to those measured using UV excimer

nanosecond laser ablation.<sup>5</sup> As shown in Fig. 3, the fractionation index for a substantial number of elements are almost unity when the laser fluence was  $1.5\text{--}3.2\ \text{J cm}^{-2}$  (using 100 fs pulses). This fractionation-index response curve shows that all elements ablate the same, as the crater is formed. For analytical chemical analysis, the sample must have the same ablation behavior, and therefore fractionation index, as the standards. If the sample ablates similarly to the standards, fractionation is not a limitation in reporting elemental ratios. Certified elements in the four NIST glasses (610, 612, 614, and 616) exhibited similar fractionation indices for femtosecond ablation at all fluences investigated. Therefore, a calibration plot can be constructed at each fluence. Fig. 4 shows a calibration curve for Pb/U ratios at a fluence of  $3\ \text{J cm}^{-2}$ . A linear correlation (slope = 1) between the measured ratios with the certified values is evident. These analytical working curves can be used for chemical analysis of samples that exhibit similar fractionation indices to the NIST glasses.

Overall, these data were surprising in that we did not expect to see a strong fractionation dependence on fluence for femtosecond laser ablation. Strong fluence dependence is regularly

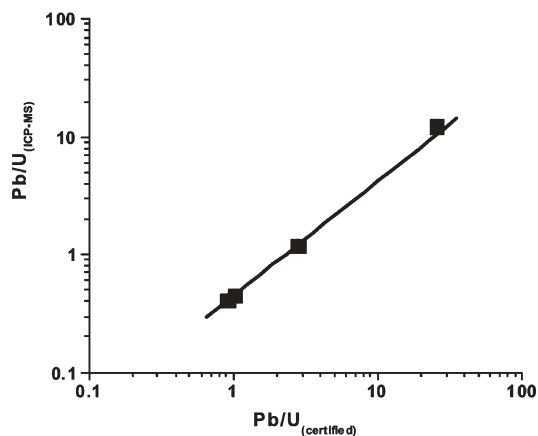
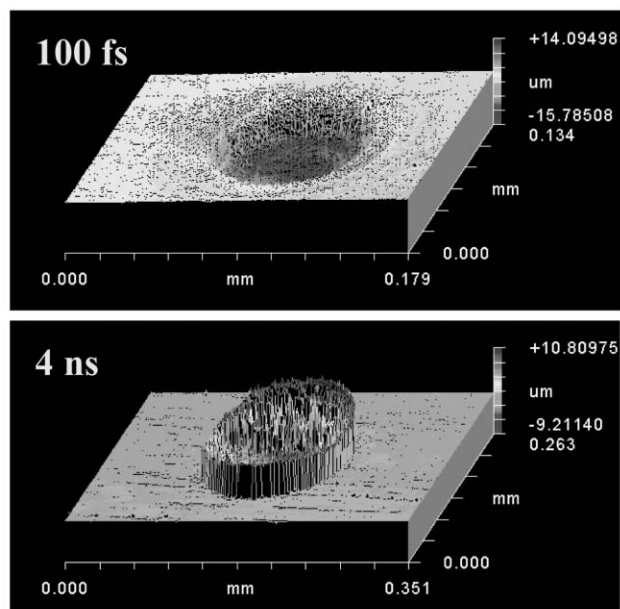


Fig. 4 Femtosecond LA-ICP-MS working curve generated using NIST 610, 612, 614, and 616 glass standards. Fluence =  $3\ \text{J cm}^{-2}$ . Plot of Pb/U ratio measured in the ICP-MS *versus* certified ratio.



**Fig. 5** Femtosecond and nanosecond pulsed laser ablated craters in metal sample.

reported for nanosecond ablation. The data reported here indicate that fractionation is not completely defined by the laser pulse duration. Other possible causes of fractionation could be the laser-induced shock wave or plasma generated at the sample surface. Recoil pressure and radiation heating of the sample surface can significantly influence mass removal. One of the most significant differences of femtosecond laser ablation is that the crater does not have a raised rim above the surface. Fig. 5 shows images of the craters generated by femtosecond and nanosecond laser pulses. The crater and surface structure for femtosecond ablation is not the same as nanosecond ablation, in which a raised rim is almost always produced. The absence of a raised rim may be a result of reduced plasma interaction or a change in the primary ejection mechanism. Nanosecond ablation involves melt-flushing that may not exist to the same extent using femtosecond laser ablation.

## Conclusion

These initial studies of laser ablation sampling with ICP-MS show that femtosecond laser pulses can be used to generate linear analytical working curves using NIST glass standards. In addition, a fluence region was found in which the fractionation indices for most of the elements in NIST glasses were one, indicating no relative fractionation as a crater is formed. These data showed similar behavior as measured using nanosecond pulses, temporal intensities of Pb, U, and the Pb/U ratio were dependent on laser fluence. It has not been established if the data measured herein are due to the 800 nm wavelength;

further work is needed to examine UV femtosecond laser ablation. UV nanosecond laser ablation is known to produce reduced fractionation related to IR nanosecond ablation. Additional research is needed to better understand femtosecond ablation and its capability for analytical chemical analysis.

## Acknowledgements

This work was supported by the US Department of Energy, Office of Basic Energy Sciences, Division of Chemical Sciences, and the Office of Nonproliferation and National Security at the Lawrence Berkeley National Laboratory under Contract No. DE-AC03-76SF00098.

## References

- 1 R. E. Russo, X. L. Mao, O. V. Borisov and H. C. Liu, in *Encyclopedia of Analytical Chemistry*, ed. R. A. Meyers, John Wiley & Sons, New York, 2000, pp. 9485–9506.
- 2 D. Günther, S. E. Jackson and H. P. Longerich, *Spectrochim. Acta, Part B*, 1999, **54**, 381.
- 3 S. F. Durrant, *J. Anal. At. Spectrom.*, 1999, **14**, 1385.
- 4 J. D. Winefordner, I. B. Gornushkin, D. Pappas, O. I. Matveev and B. W. Smith, *J. Anal. At. Spectrom.*, 2000, **15**, 1161.
- 5 D. Günther, I. Horn and B. Hattendorf, *Fresenius' J. Anal. Chem.*, 2000, **368**, 4.
- 6 R. E. Russo, X. L. Mao and O. V. Borisov, *Trends Anal. Chem.*, 1998, **17**, 461.
- 7 R. E. Russo, X. L. Mao and S. S. Mao, *Anal. Chem.*, 2002, **74**, 70A.
- 8 B. C. Stuart, M. D. Feit, S. Herman, A. M. Rubenchik, B. W. Shore and M. D. Perry, *Phys. Rev. B*, 1996, **15**, 1749.
- 9 D. Du, X. Liu, G. Korn, J. Squier and G. Mourou, *Appl. Phys. Lett.*, 1994, **64**, 3071.
- 10 L. V. Keldysh, *Sov. Phys. JETP*, 1965, **20**, 1307.
- 11 V. Margetic, K. Niemax and R. Hergenroder, *Spectrochim. Acta, Part B*, 2001, **56**, 1003.
- 12 V. Margetic, M. Bolshov, A. Stockhaus, K. Niemax and R. Hergenroder, *J. Anal. At. Spectrom.*, 2001, **16**, 616.
- 13 B. Le Droff, J. Margot, M. Chaker, M. Sabsabi, O. Barthelemy, T. W. Johnston, S. Laville, F. Vidal and Y. von Kaenel, *Spectrochim. Acta, Part B*, 2001, **56**, 987.
- 14 M. Ye and C. P. Grigoropoulos, *J. Appl. Phys.*, 2001, **89**, 5183.
- 15 V. Margetic, A. Pakulev, A. Stockhaus, M. Bolshov, K. Niemax and R. Hergenroder, *Spectrochim. Acta, Part B*, 2000, **55**, 1771.
- 16 I. Horn, R. W. Hinton, S. E. Jackson and H. P. Longerich, *Geostand. Newsl.*, 1997, **21**, 191.
- 17 N. J. G. Pearce, W. T. Perkins, J. A. Westgate, M. P. Gorton, S. E. Jackson, C. R. Neal and S. P. Chenery, *Geostand. Newsl.*, 1997, **21**, 115.
- 18 K. Hollocher and J. Ruiz, *Geostand. Newsl.*, 1995, **19**, 27.
- 19 H. C. Liu, O. V. Borisov, X. Mao, S. Shuttleworth and R. E. Russo, *Appl. Spectrosc.*, 2000, **54**, 1435.
- 20 R. Russo, X. L. Mao, O. V. Borisov and H. Liu, *J. Anal. At. Spectrom.*, 2000, **15**, 1115.
- 21 A. J. G. Mank and P. R. D. Mason, *J. Anal. At. Spectrom.*, 1999, **14**, 1143.
- 22 O. V. Borisov, X. L. Mao and R. E. Russo, *Spectrochim. Acta, Part B*, 2000, **55**, 1693.